Clay Minerals (2002) **37**, 709–718

Dedicated to Prof. Dr U. Schwertmann on the occasion of his 75th birthday

Experimental alteration of vivianite to lepidocrocite in a calcareous medium

R. ROLDÁN, V. BARRÓN AND J. TORRENT*

Departamento de Ciencias y Recursos Agrícolas y Forestales, Universidad de Córdoba, Apdo. 3048, 14080 Córdoba, Spain

(*Received 25 April 2001; revised 28 September 2001*)

ABSTRACT: Vivianite [$Fe_3(PO_4)_2{\cdot}8H_2O$] is easily oxidized in the presence of air. In this work, we studied the oxidation and incongruent dissolution of vivianite in a calcareous medium containing an anion-exchange resin (AER) that acted as a sink for phosphate. Freshly prepared vivianite suspensions with calcite sand and an AER membrane were oxidized and stirred by bubbling air or CO_2-free O_2. Experiments were finished when oxidation rate and P removal by the AER became slow, which was at 53 days (air system) or 28 days (CO_2free O_2 system). At these times, the respective values of the Fe(II)/total Fe ratio were 0.29 and 0.12, and the respective values of the atomic P/Fe ratio were 0.15 and 0.11. The final product of the oxidation was poorly crystalline lepidocrocite in the form of thin (1–5 nm), irregular lamellae that were soluble in acid oxalate. The unit-cell edge lengths of this lepidocrocite were a = 0.3117, b = 1.2572, and c = 0.3870, *vs.* a = 0.3071, b = 1.2520 and c = 0.3873 nm for the reference lepidocrocite. The lepidocrocite lamellae contained occluded P (P/Fe atomic ratio = 0.03–0.04). The results of this and a previous study made us hypothesize that this occluded P is structural and occupies tetrahedral sites adjacent to the empty octahedral sites in the sheets extending on {010}.

KEYWORDS: vivianite, lepidocrocite, Fe oxides, calcareous soils.

Vivianite, a hydrated Fe(II) phosphate of formula $Fe_3(PO_4)_2{\cdot}8H_2O$, is monoclinic-prismatic, $C2/m$ (a = 1.004 nm, b = 1.339 nm, c = 0.469 nm, β = 104º18′), and possesses a structure consisting of separate single and double octahedral groups [$FeO_2(H_2O)_4$ and $Fe_2O_6(H_2O)_4$] bonded by PO_4 groups to form sheets that extend along {010} (Kostov, 1968). Vivianite occurs as a weathering product in hydrothermal and pegmatitic deposits, and also as a secondary mineral in Fe-bearing ore veins. It also forms in a variety of reductive environments such as marine and lake sediments, and waterlogged soils, where it can limit the phosphate concentration in solution (Jensen *et al*., 1998; Hansen & Poulsen, 1999).

* E-mail: torrent@uco.es
DOI: 10.1180/0009855023740072

On exposure to air, Fe(II) in vivianite is gradually oxidized to Fe(III), the valence change being offset by replacement of H_2O with OH (McCammon & Burns, 1980). Typically, 5–10% of the Fe(II) in freshly precipitated vivianite is oxidized to Fe(III) within a few minutes if the solution is in contact with air; the conversion is accompanied by a colour change from white to light blue resulting from $Fe^{2+} \rightarrow Fe^{3+}$ charge transfer transitions. Under typical laboratory temperature and relative humidity conditions, dry vivianite is oxidized slowly: the Fe(III) concentration levels off at ~50%, the stability limit for a triclinic vivianite structure (Rouzies & Millett, 1993) after several hundred days. Fast oxidation of vivianite by hot air or hydrogen peroxide results in the formation of a poorly crystalline Fe(III) phosphate phase.

One can expect the oxidation of vivianite in an aqueous environment to result in incongruent dissolution yielding a highly insoluble Fe(III) hydr(oxide) residue and dissolved phosphate. This has in fact been the basis for using natural vivianite as a slow-release P fertilizer (Fraps, 1922; Denisova, 1973). The presence of a layer of amorphous ferric hydroxide on the cleavage surfaces of a natural specimen has been interpreted as a result of vivianite auto-oxidation (Pratt, 1997). To the authors' knowledge, no systematic laboratory experiments have to date been conducted with a view to characterizing the products of vivianite oxidation in different aqueous media. Such information would probably explain the effectiveness of vivianite as an amendment for correcting Fe deficiency in plants growing on calcareous soils (Eynard *et al*., 1992; Iglesias *et al*., 1998). According to Eynard *et al*. (1992), vivianite in aerated soils may undergo not only oxidation, but also incongruent dissolution enhanced by the presence of effective phosphate sinks (plant roots and P-sorbing soil minerals). Also, these processes may lead to the formation of ferrihydrite, which is an effective Fe source for plants (Vempati & Loeppert, 1986). The purpose of this work was to examine the artificial alteration of vivianite in an oxidizing calcareous medium and thoroughly characterize the resulting products.

MATERIALS AND METHODS

Preparation and experimental alteration of vivianite

Vivianite was prepared by adding 600 mg of $FeSO_4 \cdot 7H_2O$ to 200 mg of $(NH_4)_2HPO_4$ dissolved in 6 ml of deionized water (PO_4/Fe ratio ~0.8). This resulted in complete precipitation of dissolved Fe^{2+} and a pH $\approx$7. The suspension was centrifuged and, after removing the supernatant, the precipitate was washed several times with water until the electrical conductivity of the supernatant was <0.001 S m^{-1}. The precipitate was resuspended in 25 ml of water and then transferred to a 25 ml test tube. This suspension contained ~100 mg vivianite ml^{-1} and exhibited a light blue colour due to partial oxidation and pH ~6.

The suspension was oxidized and stirred by injecting either air or 99.99% pure oxygen at a flow rate of 2 ml s^{-1} through a polyethylene tube ($\varnothing$ = 1 mm) ending at the bottom of the test tube. The air (or oxygen) was saturated with water by passing it through two Erlenmeyer flasks filled with deionized water. The oxygen was also bubbled through 1 M NaOH to trap any CO_2. In order to buffer the medium at the typical pH of a calcareous system, 0.5 g of 0.2–0.5 mm $CaCO_3$ (calcite) sand (stirred by continuous gas bubbling) was added. The tube also contained a 5×4 cm anion exchange membrane (BDH, 55164 2S) saturated with HCO_3^- to adsorb phosphate released by vivianite. At preset times, 0.2 ml portions of the suspension were dissolved in 1 ml of 0.25 M H_2SO_4. After appropriate dilution, total Fe (Fe_t) and P (P_t) in this solution were determined using the o-phenanthroline (Olson & Ellis, 1982) and molybdenum blue (Murphy & Riley, 1962) methods, respectively. The o-phenanthroline method was also used to determine dissolved Fe(II) but, in this case, no reductant (hydroxylamine) was added. The resin membrane was replaced with a fresh one saturated with HCO_3^- on a daily basis. Used membranes were sonicated in water for 1 min to remove any adhered particles, washed with 0.5 M HCl to desorb the phosphate and then resaturated with HCO_3^- by immersing them twice in 0.5 M $NaHCO_3$. At preset times, 1 ml portions of the suspension were dried over a glass slide for mineralogical analysis. Experiments were finished when the oxidation rate dropped (viz. at Fe(II)/Fe_t ~0.2). The oxidation times were 53 and 28 days for the air and oxygen system, respectively. At the end of the experiment, the suspension was centrifuged and allowed to settle and the resulting sediment was freeze-dried for mineralogical analysis. Both experiments (air and oxygen) were done in triplicate at 294–296 K.

Mineralogical analysis of the alteration products

Powder X-ray diffraction (XRD) patterns were obtained on a Siemens D5000 instrument using Co-$K\alpha$ radiation and a graphite monochromator. Samples were scanned at 0.05 or smaller º2θ steps, using a counting time of 15 s. Crystal parameters were calculated by fitting the XRD patterns to the Rietveld equation with the aid of the GSAS software (Larson & von Dreele, 1988). The structural parameters for lepidocrocite were taken from Oles *et al*. (1970).

Micrographs of the products were obtained by using a Jeol 200CX transmission electron microscope (TEM) after depositing a drop of a dilute

suspension on a C-coated formvar film supported on a copper grid. An EDAX® energy dispersive detector fitted to a Philips 200 CM TEM was used to semiquantitatively estimate the P/Fe atomic ratio of the products. Atomic force microscopy (AFM) observations were made using a Multimode Scanning Probe Microscope (Digital Instruments) and droplets of a dilute suspension that were evaporated on a muscovite surface. To avoid artifacts, the tapping mode and an etched silicon probe were used. Gold-coated particles deposited on muscovite flakes were examined on a JEOL JSM 6300 scanning electron microscope (SEM).

Colour was determined with a Varian Cary 1E spectrophotometer equipped with a diffuse reflectance attachment. Reflectance (R) values were obtained at 0.5 nm intervals over the 350–900 nm range and converted to Munsell notation (Barrón & Torrent, 1986). The position of each absorption band in the visible region was determined from the minimum in the second-derivative curve of the Kubelka–Munk function $[(1 - R)^2/2R]$, which was obtained by applying a cubic spline fitting procedure to a series of 30 consecutive R values (Scheinost *et al*., 1998). Infrared spectra of KBr pellets containing 1 mg of sample in 200 mg of KBr were recorded from 380 to 4000 cm^{-1} on a Perkin-Elmer 2000 FTIR spectrophotometer using 4 cm^{-1} resolution and an average of 100 scans.

Acid oxalate-soluble Fe in the products was determined according to Schwertmann (1964).

RESULTS

Chemical changes during alteration

The pH of the suspensions was effectively buffered by $CaCO_3$ during oxidation, with values of 8.25±0.05 and 8.95±0.1 in the air and oxygen treatment, respectively. The oxidation rate as measured by the rate of change in the $Fe(II)/Fe_t$ ratio of the suspension was significantly higher in oxygen than in air (Fig. 1). The difference can be ascribed to higher O_2 activity and pH in the former, but which factor is more influencial cannot be ascertained.

The P_t/Fe_t atomic ratio at the beginning of the experiments, 0.7, was close to the theoretical value for unaltered vivianite (0.67). It decreased in a manner similar to the $Fe(II)/Fe_t$ ratio. Final values were 0.16 for the air and 0.10 for the oxygen system, respectively (Fig. 2). The resin membranes were thus effective in removing phosphate from the solution. The rate of phosphate removal probably did not restrict the rate of vivianite dissolution because the amount of P adsorbed by the resin was much less than the measured anion exchange capacity of the membrane (0.45 $mmol_c$ $membrane^{-1}$) in all cases.

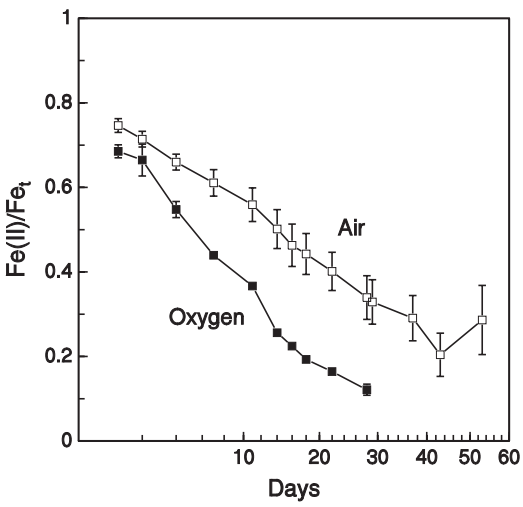

FIG. 1. Variation of the $Fe(II)/Fe_t$ ratio in vivianite as a function of time for suspensions oxidized with air and oxygen. A square-root time scale is used to show that the oxidation kinetics conform to a parabolic diffusion law.

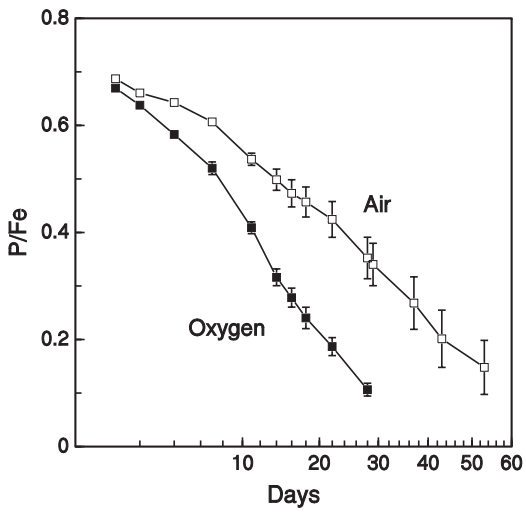

FIG. 2. Variation of the P_t/Fe_t atomic ratio in vivianite as a function of time for suspensions oxidized with air and oxygen. A square-root time scale is used to show that the kinetics of P loss conform to a parabolic diffusion law.

Both oxidation and loss of P from the solid phase conformed to a parabolic diffusion law, as suggested by the roughly straight lines obtained by plotting Fe(II)/Fe_t and P_t/Fe_t against the square root of time (Figs 1 and 2). This type of kinetics may indicate that the rate-limiting process is intra- or interparticle diffusion (Sparks, 1988), where electron carriers and phosphate ions are the diffusing species.

Oxidation products

Temporal changes in the chemical composition of the suspension reflected substantial changes in the mineralogical nature of the solid products. Such changes were similar in all experiments, so only data for one of the experiments with oxygen are reported.

The XRD patterns (Fig. 3) exhibit a gradual decrease in the intensity of the vivianite reflections and the appearance of reflections typical of lepidocrocite, which was the only crystalline phase detected at the end of the experiment. The fitting by Rietveld analysis of the XRD traces of the lepidocrocite was good, as suggested by a 2.87 value of the $(R_{wp}/R_{exp})^2$ parameter (Bish, 1993) (R_{wp} = weighted profile residual = 4.23; R_{exp} = expected residual = 2.50; with perfect refinement, R_{wp}/R_{exp} = 1). The lattice parameters for the orthorhombic lepidocrocite are a = 0.3117 nm, b = 1.2572 nm and c = 0.3870 nm, *vs.* values of 0.3071 nm, 1.2520 nm and 0.3873 nm, respectively, for the reference lepidocrocite (JCPDS Card 44–1415).

The light blue (4.4B 5.2/1.8) colour typical of vivianite gradually changed to the yellowish red (5.1YR 5.2/6.0) typical of lepidocrocite (Cornell & Schwertmann, 1996). The second derivative of the Kubelka-Munk function for the starting vivianite exhibited, in agreement with the data of Amthauer & Rossman (1984), absorption bands at 445 nm (spin-forbidden Fe^{2+} transition), at a zone around

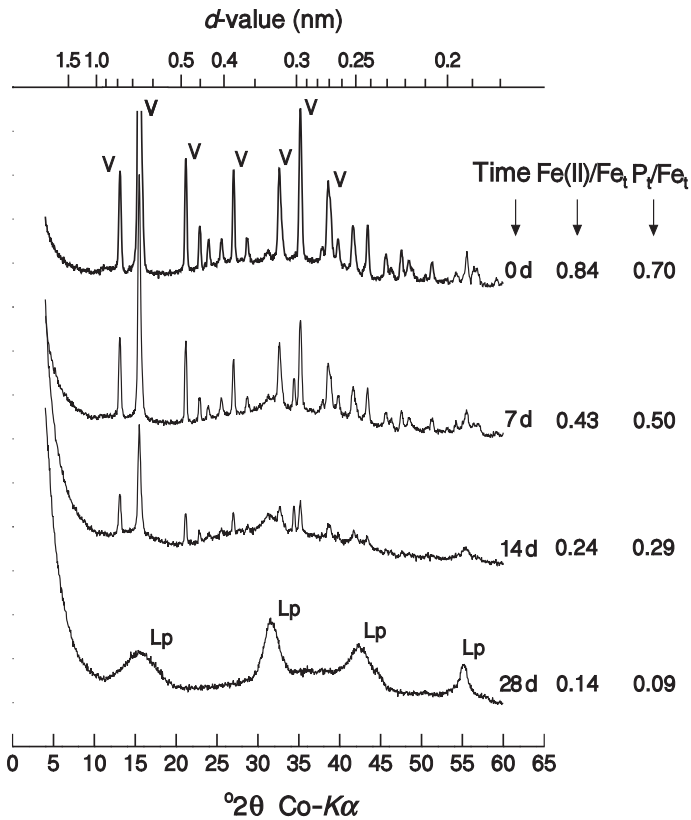

FIG. 3. XRD patterns of the products obtained after progressive oxidation of the vivianite suspension with oxygen. The oxidation time is stated to the right of each pattern. The pattern for 0 days corresponds to the vivianite suspension immediately before oxidation with oxygen.

630 nm ($Fe^{2+} \rightarrow Fe^{3+}$ intervalence charge transfer), and at 880 nm (Fe^{2+} crystal field transition) (Fig. 4a). By contrast, the final product exhibited the lepidocrocite bands at 425 nm ($^6A_1 \rightarrow {}^4E$; $^4A_1$ single electron transition) and 485 nm [$2(^6A_1) \rightarrow 2(^4T_1)$ electron pair transition] (Scheinost *et al*., 1998), with no evidence of superimposed vivianite bands (Fig. 4b).

The vivianite IR spectrum (Fig. 5a) exhibits H_2O-related bands at 826 cm^{-1} (rock) and 556–450 cm^{-1} (bend), and PO_4 (stretch) bands at 1042–971 cm^{-1}, consistent with those for near-ideal, slightly oxidized specimens (Rodgers, 1987). As oxidation develops, the lepidocrocite bands at 1089, 1022 and 742 cm^{-1} (OH-bend) and 547–470 cm^{-1} (Fe-O stretch) become apparent (Fig. 5b–d). The origin of the two well-defined bands at 1260 and 805 cm^{-1} is uncertain; however, they might be related to the presence of structural PO_4 in lepidocrocite (as discussed later on). The former appears to be at the upper limit of the PO_4 antisymmetric stretch for some phosphates, whereas the latter occurs as an out-of-plane OH bend in some phosphates containing OH or water (Ross, 1974).

The SEM showed the starting vivianite to consist of imperfectly rhomboidal to spindle-shaped crystals (length, 3–15 μm; width, 1–5 μm; thickness, 0.3–1 μm) flattened along {010} and usually occurring in radiated aggregates (Fig. 6a). In the course of alteration, the aggregates and individual crystals gradually lost their sharp edges and shrank (Fig. 6b). Eventually, they became irregular masses of <5 μm (Fig. 6c) that were easily dispersed in water upon sonication. The TEM images for the final products (Fig. 7) exhibit thin, irregular lamellae of variable width (20–100 nm) that are partly folded. As can be seen from Fig. 8, the lamellae ranged from ~1 to 5 nm (i.e. from one to four unit cells) in thickness as estimated with the AFM. This is consistent with the large full width at half maximum (FWHM) of the XRD peaks and also with the complete dissolution of the final product in acid oxalate, which is typical of poorly crystalline lepidocrocite (Cumplido *et al*., 2000). The P/Fe atomic ratio of these lepidocrocite particles, as estimated by energy dispersive analysis ranged from 0.03 to 0.04.

DISCUSSION

Phosphate hinders or suppresses the formation of crystalline Fe oxides (Cornell & Schwertmann, 1996), probably because their precursors (e.g. green rust in Fe(II) systems or ferrihydrite in Fe(III) systems) readily adsorb phosphate ions. However, Cumplido *et al*. (2000) found the oxidation of Fe(II) sulphate in the presence of phosphate to result in the formation of poorly crystalline lepidocrocite, in contrast to a mixture of well crystallized goethite (dominant) and lepidocrocite in the P-free system. These authors suggested that, because lepidocrocite is less dense than goethite, it may accommodate interlayer phosphate contained in the precursor green rust better than goethite. In Fe(III) sytems, poorly crystalline lepidocrocite was the only crystalline Fe oxide

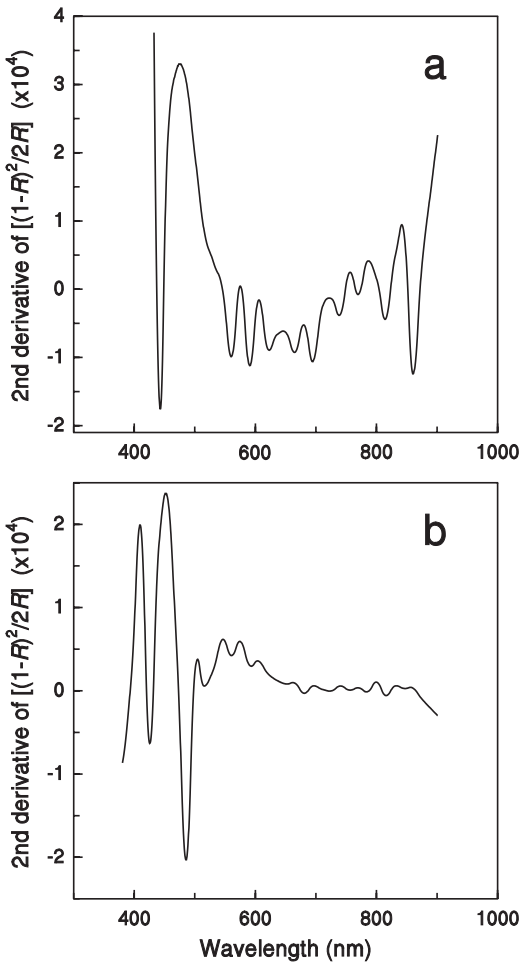

FIG. 4. Second-derivative diffuse reflectance spectrum for (a) the starting vivianite and (b) the product (mostly lepidocrocite) obtained upon oxidation with oxygen for 28 days.

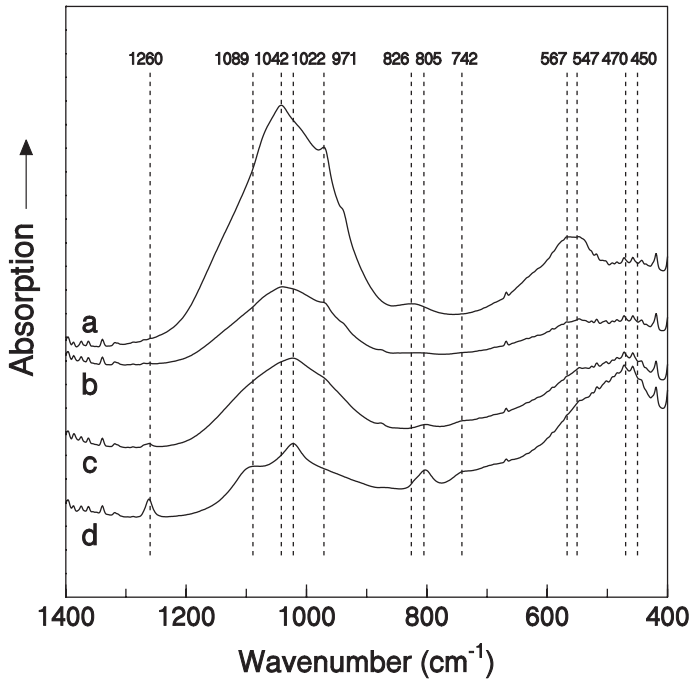

FIG. 5. Infrared spectra in the 400–1400 cm^{-1} range for the starting vivianite (a) and the products obtained upon oxidation with oxygen for 7 days (b), 14 days (c) and 28 days (d). See text for assignation of marked bands.

formed at P/Fe >0.025 (Gálvez *et al*., 1999). The alteration of vivianite to lepidocrocite is thus consistent with this 'pro-lepidocrocitic' effect of phosphate. The formation of lepidocrocite was probably favoured by the removal of excess phosphate by the AER; this left little phosphate available to block the rearrangement of the $Fe(OH)_6$ polyhedra into an ordered phase.

The results of our experiments are inconclusive with regard to the specific mechanism by which lepidocrocite is formed from vivianite. The similarity between the structures of the two minerals suggests that internal rearrangement processes in oxidized, P-depleted vivianite could lead to the formation of lepidocrocite. Specifically, the single and double FeO_6 octahedra running along [100] and [010] in vivianite might coalesce to form the corrugated octahedral sheets that extend on {010} in lepidocrocite (Fig. 9). This obviously entails the removal of most PO_4 groups in vivianite.

It is difficult to ascertain whether it is phosphate or HCO_3^-/CO_3^{2-} in solution which is the main factor responsible for the small size of the lepidocrocite crystals. Carlson & Schwertmann (1990) found that an increasing concentration of HCO_3^- resulted in increasing width of the XRD reflections for the lepidocrocite produced from Fe(II) salts. On the other hand, Cumplido *et al*. (2000) reported a strong increase in line width with increasing P concentration at the same HCO_3^- concentration. Therefore, it seems likely that both factors contribute to the poor crystallinity observed in the present work.

The concentration of Fe(II) in the end product indicates that some vivianite remains unaltered – despite the absence of vivianite reflections in the XRD pattern and vivianite bands in the second derivative reflectance spectrum. Therefore, part of the P of the product must be assigned to the residual vivianite. However, the lepidocrocite lamellae also contain P, with a P/Fe ratio of 0.03–0.04, as indicated before. Because the AER is expected to have removed most of the phosphate adsorbed on the lepidocrocite surface, that P is likely to be in an occluded form. Cumplido *et al*. (2000), who synthesized lepidocrocite from phosphate-containing Fe(II) sulphate solutions, suggested that phosphate occluded in lepidocrocites might be structural. The results of these authors are similar to those of the present study because

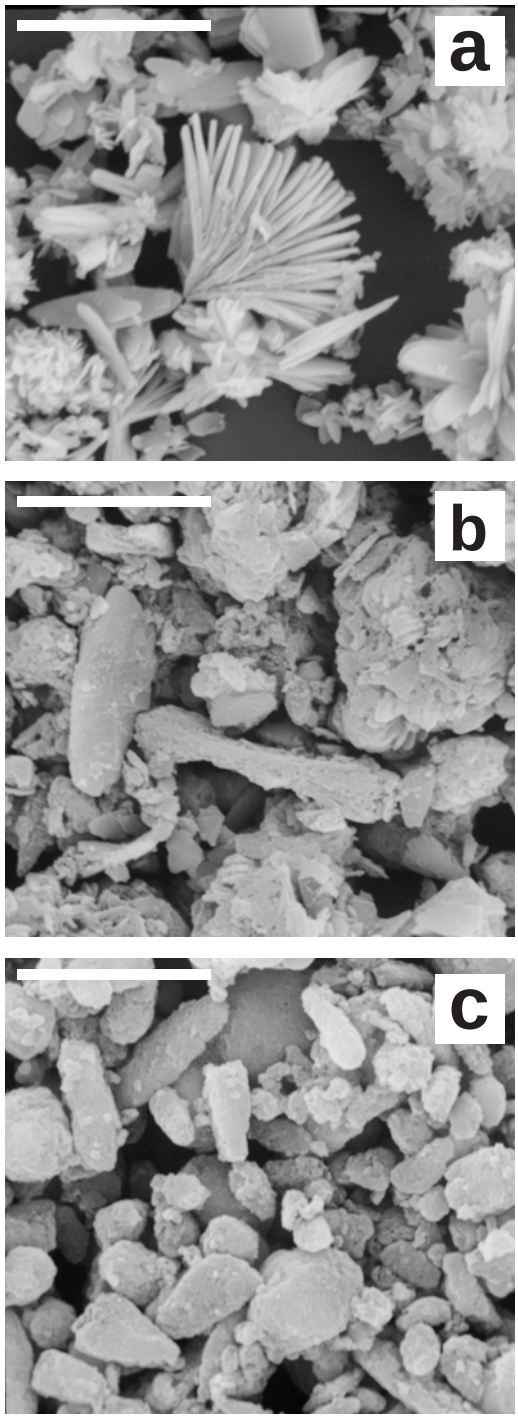

FIG. 6. SEM images of the starting vivianite (a) and the products obtained by oxidizing it with oxygen for 14 days (b) and 28 days (c). Scale bar = 10 μm.

FIG. 7. TEM image of the lepidocrocite obtained by oxidizing vivianite with oxygen for 28 days. Scale bar = 100 nm.

increasing P content resulted in significant increases in the *a* unit-cell edge length and unit-cell volume, and, as indicated before, in broadening of the XRD reflections.

We put forward the hypothesis that, if present, structural P in lepidocrocite might occupy the tetrahedral sites intercalated in the double rows of empty octahedral sites that run parallel to the *c* axis and form sheets on {010} (Fig. 10). The O–O distance in the PO_4 tetrahedron in phosphates is ~0.26 nm and hence shorter than the distances between the four O atoms (labelled 1 to 4) pertaining to the tetrahedron of Fig. 10 (0.306 nm for O_1–$O_{2,3}$, 0.307 nm for O_2–O_3, 0.265 nm for O_1–O_4, and 0.392 nm for $O_{2,3}$–O_4). Accommodation of P in the lepidocrocite structure would require these distances to become similar, which would in turn result in changes in the unit-cell parameters. As indicated before, such changes are observed in the lepidocrocites studied by Cumplido *et al*. (2000) and in the ones described in this work. The net outcome of an increase in the *a* and little changes in the *b* and *c* unit-cell edge lengths is a

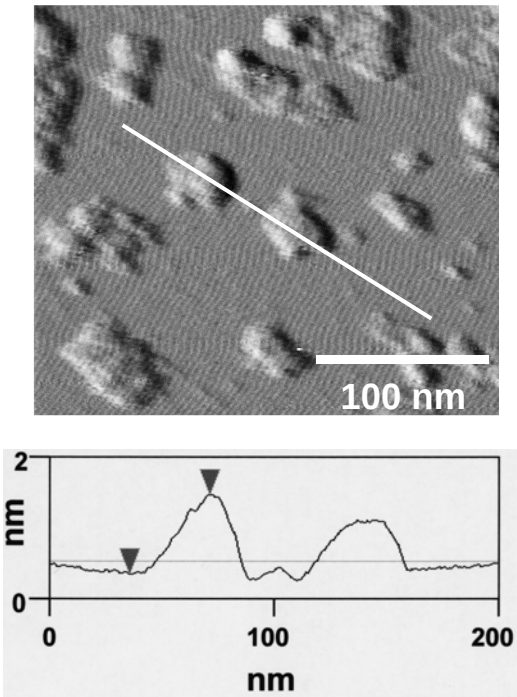

FIG. 8. AFM image of well-dispersed particles of the lepidocrocite obtained by oxidizing vivianite with oxygen for 28 days. The cross-section corresponds to the line marked on the image.

small increase in the volume of the unit cell from 0.1489 nm^3 for the reference lepidocrocite to 0.1517 nm^3 for the above-described lepidocrocite.

CONCLUSIONS

Lepidocrocite was the only crystalline Fe oxide detected after the experimental oxidation of vivianite in a calcareous medium containing a phosphate sink. This lepidocrocite occurs as thin irregular lamellae, exhibits broad XRD reflections, is completely soluble in acid oxalate and contains occluded P. The unit-cell edge lengths of lepidocrocite suggest that this P might be structural. It is hypothesized that the P atoms might occupy the tetrahedral sites adjacent to the empty octahedral sites in the sheets that extend on {010}. The potential alteration of vivianite to poorly crystalline lepidocrocite in calcareous environments may explain why vivianite is an effective amendment to alleviate Fe deficiency in plants growing on calcareous soils.

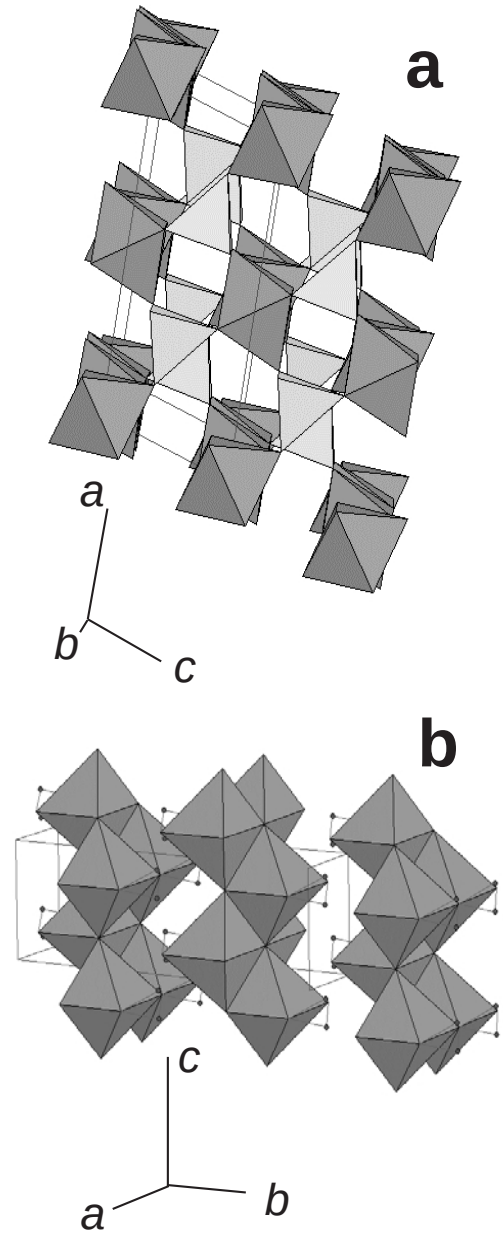

FIG. 9. Structures of (a) vivianite and (b) lepidocrocite. Shaded octahedra and tetrahedra are filled with Fe and P atoms, respectively.

ACKNOWLEDGMENTS

This work was supported by Projects OLI96-2183 (CICYT, Spain) and PB98-1015 (Ministerio de Educación y Ciencia, Spain). The authors wish to thank Prof. M.A. Aramendía and Mr A. Marinas,

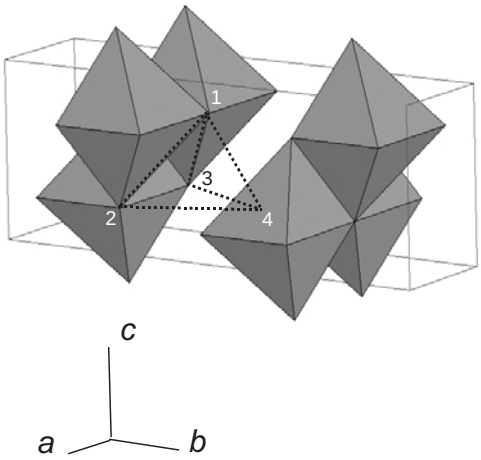

FIG. 10. Model for lepidocrocite with structural P where the P atoms occupy tetrahedral sites adjacent to the double rows of octahedra that form sheets on {010}. The distances between the four oxygen atoms (marked 1 to 4) surrounding the tetrahedral site in the undistorted lepidocrocite structure are 0.306 nm for $O_1-O_{2,3}$, 0.307 nm for O_2-O_3, 0.265 nm for O_1-O_4 and 0.392 nm for $O_{2,3}-O_4$.

Departamento de Química Orgánica, Universidad de Córdoba, for their assistance with the IR analyses, and Ms C. Rojas, Instituto de Ciencia de los Materiales, Sevilla, for carrying out the energy dispersive spectrometry analyses.

REFERENCES

Amthauer G. & Rossman G.R. (1984) Mixed-valence of iron in minerals with cation clusters. *Physics and Chemistry of Minerals*, **11**, 37–51.

Barrón V. & Torrent J. (1986) Use of the Kubelka–Munk theory to study the influence of iron oxides on soil colour. *Journal of Soil Science*, **37**, 499–510.

Bish D.L. (1993) Studies of clays and clay minerals using X-ray powder diffraction and the Rietveld method. Pp. 79– 21 in: *Computer Applications to X-ray Diffraction Analysis of Clay Minerals* (R.C. Reynolds & J.R. Walker, editors). The Clay Minerals Society, Boulder, Colorado, USA.

Carlson L. & Schwertmann U. (1990) The effect of CO_2 and oxidation rate on the formation of goethite versus lepidocrocite from an Fe(II) system at pH 6 and 7. *Clay Minerals*, **25**, 65–71.

Cornell R.M. & Schwertmann U. (1996) *The Iron Oxides.* VCH, Weinheim, Germany.

Cumplido J., Barrón V. & Torrent J. (2000) Effect of phosphate on the formation of nanophase lepidocrocite from Fe(II) sulfate. *Clays and Clay Minerals*, **48**, 503–510.

Denisova N.V. (1973) Use of peat vivianite on leached chernozems of western Siberia. *Agrokhimiya*, **1**, 87–91.

Eynard A., del Campillo M.C., Barrón V. & Torrent J. (1992) Use of vivianite ($Fe_3(PO_4)_2{\cdot}8H_2O$) to prevent iron chlorosis in calcareous soils. *Fertilizer Research*, **31**, 61–67.

Fraps G.S. (1922) *Availability of some nitrogenous and phosphatic materials*. Texas Agricultural Experimental Station Bulletin 285.

Gálvez N., Barrón V. & Torrent J. (1999) Effect of phosphate on the crystallization of hematite, goethite, and lepidocrocite from ferrihydrite. *Clays and Clay Minerals*, **47**, 304–311.

Hansen H.C.B. & Poulsen I.F. (1999) Interaction of synthetic sulfate green rust with phosphate and the crystallization of vivianite. *Clays and Clay Minerals*, **47**, 312–318.

Iglesias I., Dalmau R., Marcé X., del Campillo M.C., Barrón V. & Torrent J. (1998) Diversos fosfatos de hierro presentan eficacia prolongada en la prevención de la clorosis férrica en peral (cv. Blanquilla). *Fruticultura Profesional*, **99**, 76–87.

Jensen M.B., Hansen H.C.B., Nielsen N.E. & Magid J. (1998) Phosphate mobilization and immobilization in 2 soils incubated under simulated reducing conditions. *Acta Agricultura Scandinavica, Section B*, **48**, 11–17.

Kostov I. (1968) *Mineralogy*. Oliver and Boyd, Edinburgh, UK.

Larson A.C. & von Dreele R.B. (1988) *GSAS. Generalized structure and analysis systems: Los Alamos National Laboratory Report LAUR 86-748*. Los Alamos National Laboratory, New Mexico, USA.

McCammon C.A. & Burns R.G. (1980) The oxidation mechanism of vivianite as studied by Mössbauer spectroscopy. *American Mineralogist*, **65**, 361–366.

Murphy J. & Riley J.P. (1962) A modified single solution method for the determination of phosphate in natural waters. *Analitica Chimica Acta*, **27**, 31–36.

Oles A., Szytula A. & Wanic A. (1970) Neutron diffraction study of γ-FeOOH. *Physica Status Solidi*, **41**, 173–177.

Olson R.V. & Ellis R., Jr. (1982) Iron. Pp. 301–312 in: *Methods of Soil Analysis. Part 2*. 2nd edition (A.L. Page, R.H. Miller & D.R. Keeney, editors). Agronomy Society of America and the Soil Science Society of America, Madison, Wisconsin, USA.

Pratt A.R. (1997) Vivianite auto-oxidation. *Physics and Chemistry of Minerals*, **25**, 24–27.

Rodgers K.A. (1987) Baricite, a further occurrence.

Neues Jahrbuch für Mineralogie Monatshefte, 183–192.

Ross S.D. (1974) Phosphate and other oxy-anions of Group V. Pp. 383–422 in: *The Infrared Spectra of Minerals* (V.C. Farmer, editor). Monograph **4**, Mineralogical Society, London.

Rouzies D. & Millet J.M.M. (1993) Mössbauer study of synthetic oxidized vivianite at room temperature. *Hyperfine Interactions*, **77**, 19–28.

Scheinost A.C., Chavernas A., Barrón V. & Torrent J. (1998) Use and limitations of second-derivative diffuse reflectance spectroscopy in the visible to near-infrared range to identify and quantify Fe oxides in soils. *Clays and Clay Minerals*, **46**, 528–536.

Schwertmann U. (1964) Differenzierung der Eisenoxide des Bodens durch Extraktion mit sauer Ammoniumoxalat-Lösung. *Zeitschrift für Pflanzenernährung, Düngung und Bodenkunde*, **105**, 194–202.

Sparks D.L. (1988) *Kinetics of Soil Chemical Processes*. Academic Press, San Diego, California, USA.

Vempati R.K. & Loeppert R.H. (1986) Synthetic ferrihydrite as a potential iron amendment in calcareous soils. *Journal of Plant Nutrition*, **9**, 1039–1052.